

# An Algorithm to Estimate Manipulator Dynamics Parameters'

Pradeep K. **khosla** and Takeo **kanade**

Department of Electrical and Computer Engineering  
The Robotics Institute  
Carnegie-Mellon University  
Pittsburgh, PA 15213

## Abstract

This paper presents algorithms for identifying parameters of **an** N degrees-of-freedom robotic manipulator. First, we outline the fundamental properties of the Newton-Euler formulation of robot dynamics from the view point of parameter identification. We then show that the Newton-Euler model which is nonlinear in the dynamic parameters can **be** transformed into **an** equivalent modified model which is linear in dynamic parameters. We develop both on-line and off-line parameter estimation procedures. To illustrate our approach, we identify the dynamic parameters of the cylindrical robot, **and** the three degree-of-freedom positioning system of the CMU Direct-Drive Arm II. The experimental implementation of our algorithm to estimate the dynamics parameters of the **six** degrees-of-freedom CMU DD Arm II is also presented.

## 1. Introduction

The robot control problem centers around the computation of the actuating torques/forces to produce the desired motion of the end-effector. The model-based control schemes such as the computed-torque [14] and resolved-acceleration [12] controllers accomplish this objective by incorporating the complete dynamic model of the manipulator in the control law. Since the fundamental assumption here is that the robot dynamics are modeled accurately, precise knowledge of the kinematic and dynamic parameters of the robot is required. In practice, it is **also** necessary to identify on-line the mass and inertial characteristics of the payload in order to achieve accurate trajectory tracking with varying payload.

This paper presents an algorithm to estimate the dynamics parameters of a robot from the measurements of its inputs (actuating torques/forces) and outputs (joint positions, velocities and accelerations). To facilitate the identification procedure, we modify the Newton-Euler formulation so that it becomes linear in the dynamic parameters. We introduce the torque/force error model for parameter identification based on this modified Newton-Euler formulation of the robot dynamics. The torque/force error model is then cast into the series (input-error) and parallel (outputerror) identifier structures for on-line and off-line parameter estimation, respectively.

Earlier work in identification of robot dynamics concentrated on estimating the mass of the payload. Paul [16] presented two techniques with the assumption that the manipulator is at rest. His first method used the joint torques/forces, and the second method a wrist torque/force sensor. Coiffet [4] extended this technique, for a manipulator at rest, to estimate **also** the center-of-mass of the payload. By using special test torques and moving only one degree-of-freedom at a time, the moments-of-inertia of the payload can also be estimated. Recently, general purpose algorithms to estimate the dynamics parameters have been proposed [9, 15, 1].

Our general-purpose algorithm is suited for both on-line and off-line applications: in off-line identification only one link of the robot is commanded to move for the purpose of parameter estimation, whereas in on-line identification the parameters are estimated while the robot is in motion performing the task in hand. We **can** adopt the strategy of estimating off-line the dynamics parameters of the robot and then estimating on-line the inertial characteristics of the payload. This procedure improves the robustness of the estimation, decreases the computational requirements, and adapts to varying payloads. We demonstrate our identification algorithm through simulation experiments **on** a cylindrical robot, and the positioning system (i.e., the first three degrees-of-freedom) of the CMU Direct-Drive Arm II [7]. We have implemented our identification algorithm to estimate the dynamics parameters of the six degrees-of-freedom **CMU** DD Arm II and the experimental results are presented in this paper.

This paper is organized as follows: In Section 2, we review the Newton-Euler formulation and identify its properties applicable to robot parameter identification. We then derive, in Section 3, our identification procedures for a general-purpose  $N$  degree-of-freedom robot. In Section 4, we evaluate the performance of our algorithm on the two case study robots. The experimental results for the six degrees-of-freedom CMU DD Arm II are presented in Section 5 and finally, in Section 6, we draw our conclusions.

## 2. Properties of Robot Dynamics Model for Parameter Estimation

Robot dynamics describe the temporal interactions of the joint motions in response to the inertial, centrifugal, Coriolis, gravitational, and actuating torques/forces. Robot dynamics are highly coupled and nonlinear second-order differential equations. The identification problem is to estimate all of the kinematic and dynamic parameters that affect the link torques/forces. The Denavit-Hartenberg parameters constitute the kinematic parameters, and the link masses, link inertias, and center-of-mass vectors are the dynamic parameters.

Two formulations have been used to model robot dynamics [16, 2,13]: closed-form Lagrange formulation and recursive Newton-Euler formulation. While the former leads to physical insight, the latter is computationally more efficient and suited for real-time control applications. We will base our development of parameter identification algorithms on the Newton-Euler formulation. We first summarize the  $O(N)$  recursive Newton-Euler dynamic equations and show that it is nonlinear in the dynamic and kinematic parameters. We then show that transforming the classical link inertia tensor (expressed about the center of mass of the link) to the link coordinate frame results in a modified Newton-Euler formulation which is linear in all dynamic parameters. This modified linear formulation is more attractive from the identification point-of-view.

### 2.1. Newton-Euler Formulation

The Newton-Euler formulation shown in equations (1)-(9) computes the inverse dynamics (ie., joint torques/forces from joint positions, velocities, and accelerations) based on two sets of recursions: the forward and *backward* recursions. The forward recursions (1)-(4) transform the kinematic variables from the base to the end-effector. The initial conditions (for  $i=0$ ) assume that the manipulator is at rest in the gravitational field. The backward recursions (5)-(9) transform the forces and moments from the end-effector to the base, and culminate with the calculation of the joint torques/forces.

$$\omega_{i+1} = \begin{cases} \mathbf{A}_{i+1}^T [\omega_i + \mathbf{z}_o \dot{\theta}_{i+1}] & \text{rotational} \\ \mathbf{A}_{i+1}^T \omega_i & \text{translational} \end{cases} \quad (1)$$

$$\dot{\omega}_{i+1} = \begin{cases} \mathbf{A}_{i+1}^T [\dot{\omega}_i + \mathbf{z}_o \dot{\theta}_{i+1} + \omega_i \times (\mathbf{z}_o \dot{\theta}_{i+1})] & \text{rotational} \\ \mathbf{A}_{i+1}^T \dot{\omega}_i & \text{translational} \end{cases} \quad (2)$$

$$\mathbf{v}_{i+1} = \begin{cases} \mathbf{A}_{i+1}^T \dot{\mathbf{v}}_i + \dot{\omega}_{i+1} \times \mathbf{p}_{i+1} + \omega_{i+1} \times (\omega_{i+1} \times \mathbf{p}_{i+1}) & \text{rotational} \\ \mathbf{A}_{i+1}^T [\dot{\mathbf{v}}_i + \mathbf{z}_o \ddot{d}_{i+1} + 2\omega_i \times (\mathbf{z}_o \dot{d}_{i+1})] \\ + \dot{\omega}_{i+1} \times \mathbf{p}_{i+1} + \omega_{i+1} \times (\omega_{i+1} \times \mathbf{p}_{i+1}) & \text{translational} \end{cases} \quad (3)$$

$$\omega_0 = \dot{\omega}_0 = \mathbf{v}_0 = \mathbf{0}$$

$$\dot{\mathbf{v}}_0 = [g_x \ g_y \ g_z]^T \quad \text{gravitational acceleration}$$

$$\dot{\mathbf{v}}_i^* = \dot{\omega}_i \times \mathbf{s}_i + \omega_i \times (\omega_i \times \mathbf{s}_i) + \dot{\mathbf{v}}_i \quad (4)$$

$$\mathbf{F}_i = m_i \dot{\mathbf{v}}_i^* \quad (5)$$

$$\mathbf{N}_i = \mathbf{I}_i \dot{\omega}_i + \omega_i \times (\mathbf{I}_i \omega_i) \quad (6)$$

$$\mathbf{f}_i = \mathbf{A}_{i+1} \mathbf{f}_{i+1} + \mathbf{F}_i \quad (7)$$

$$\mathbf{n}_i = \mathbf{A}_{i+1} \mathbf{n}_{i+1} + \mathbf{p}_i \times \mathbf{f}_i + \mathbf{N}_i + \mathbf{s}_i \times \mathbf{F}_i \quad (8)$$

$$\tau_i = \begin{cases} \mathbf{n}_i^T (\mathbf{A}_i^T \mathbf{z}_o) & \text{rotational} \\ \mathbf{f}_i^T (\mathbf{A}_i^T \mathbf{z}_o) & \text{translational} \end{cases} \quad (9)$$

$\mathbf{f}_{N+1}$ : external force at the end-effector.

$\mathbf{n}_{N+1}$ : external moment at the end-effector.

The computational requirements of the general-purpose and customized recursive Newton-Euler algorithms for various types of manipulators, such as manipulators with parallel/perpendicular joint axes, spherical wrists, or sparse center-of-mass vectors and inertia tensors, have been detailed in [7].

From equations (1)-(9), we note the following properties:

1. The Newton-Euler model is **linear** in the classical link inertia tensors  $\mathbf{I}_i$ .

This property follows directly from the backward recursions in (5)-(9). The joint torque/force  $\tau_i$  in (9) is linear in the moment  $\mathbf{n}_i$ . In the recursion for the moment  $\mathbf{n}_i$  in (8), the net moment  $\mathbf{N}_i$  exerted on link  $i$  appears additively. Finally, the moment  $\mathbf{N}_i$

---

 Table 1: Kinematic and Dynamic Parameters

$m_i$	Total mass of link $i$
$\tau_i$	Joint torque/force at joint $i$
$\omega_i$ and $\dot{\omega}_i$	Angular velocity and acceleration of the $i$ -th coordinate frame
$v_i$ and $\dot{v}_i$	Linear velocity and acceleration of the $i$ -th coordinate frame
$v_i^*$ and $\dot{v}_i^*$	Linear velocity and acceleration of the center-of-mass of link $i$
$F_i$ and $N_i$	Net force and moment exerted on link $i$
$f_i$ and $n_i$	Force and moment exerted on link $i$ by link $i-1$
$p_i$	Position of the $i$ -th coordinate frame with respect to the $(i-1)$ -th coordinate frame: $p_i = [a_i, d_i, \sin\alpha_i, d_i \cos\alpha_i]^T$
$s_i$	Position of the center-of-mass of link $i$ : $s_i = [s_{ix}, s_{iy}, s_{iz}]^T$
$z_0$	$= [0 \ 0 \ 1]^T$
$A_i$	Orthogonal rotation matrix which transforms a vector in the $i$ -th coordinate frame to a coordinate frame which is parallel to the $(i-1)$ -th coordinate frame:
	$A_i = \begin{bmatrix} \cos\theta_i & -\cos\alpha_i \sin\theta_i & \sin\alpha_i \sin\theta_i \\ \sin\theta_i & \cos\alpha_i \cos\theta_i & -\sin\alpha_i \cos\theta_i \\ 0 & \sin\alpha_i & \cos\alpha_i \end{bmatrix}$
	for $i=1,2, \dots, N$ , where $A_{N+1} \triangleq E$ .
$I_i$	Classical inertia tensor of link $i$ about the center-of-mass of link $i$ (and parallel to the $i$ -th coordinate frame); with principal inertias $I_{ixx}$ , $I_{yy}$ and $I_{zz}$ ; and cross-inertias $I_{xy}$ , $I_{yz}$ and $I_{xz}$ .

---

in (6) is linear in the classical link inertia tensor  $\mathbf{I}_i$ .

2. For rotational joints, the Newton-Euler model is *nonlinear* in the center-of-mass vectors  $\mathbf{s}_i$ .

From (4) and (5), the net force  $\mathbf{F}_i$  is linear in the center-of-mass vector  $\mathbf{s}_i$ . The vector cross product  $\mathbf{s}_i \times \mathbf{F}_i$  in (8) is thereby nonlinear (quadratic) in  $\mathbf{s}_i$ . Hence, the torque  $\tau_i$  for a rotational joint in (9) is nonlinear in the center-of-mass vector  $\mathbf{s}_i$ . It must be noted that for translational joints the center-of-mass vectors appear linearly.

3. The Newton-Euler model is *nonlinear* in the kinematic parameter vectors  $\mathbf{p}_i$ .

From (3)-(5) and (7), the link force  $\mathbf{f}_i$  is linear in the vector,  $\mathbf{p}_i$ . The vector cross product  $\mathbf{p}_i \times \mathbf{f}_i$  in (8) is thereby nonlinear in  $\mathbf{p}_i$ . Hence, the torque/force  $\tau_i$  in (9) is nonlinear in the vector,  $\mathbf{p}_i$ .

4. The dynamic equations of links  $i+1$  through  $N$  are independent of the mass  $m_i$  and the classical inertia tensor  $\mathbf{I}_i$  of link  $i$ .

This physically intuitive property is an immediate consequence of the backward recursions.

In summary, the classical link inertia tensors  $\mathbf{I}_i$  and the link masses  $m_i$  appear linearly in the Newton-Euler dynamics model, but the link masses are multiplied by linear and/or quadratic functions of the center-of-mass vectors  $\mathbf{s}_i$  and nonlinear functions of the joint position variables  $\theta_i$ . In contrast, the Lagrange formulation, which utilizes the pseudo-inertia matrices, has been shown to be linear in the dynamic parameters [15]. The pseudo-inertia matrices are formed by first expressing the classical inertia tensors about the link coordinate frames and then combining their elements linearly. We thus infer that if the Newton-Euler model in (1)-(9) is reformulated such that the link inertia tensors are expressed about the link coordinate frames instead of the link center-of-mass coordinate frame, the modified Newton-Euler formulation will be also linear in the center of the mass vectors  $\mathbf{s}_i$ .

## 2.2. Transformation of Inertia Tensor

Let  $C_i = (x_i, y_i, z_i)$  be a Denavit-Hartenberg coordinate frame for link  $i$  and let  $C_i^* = (x_i^*, y_i^*, z_i^*)$  be a coordinate frame which is fixed at the center-of-mass of link  $i$  and whose axes are parallel with those of  $C_i$ . From the definition,  $\mathbf{s}_i$  is the translational vector from the origin of the link coordinate frame  $C_i$  to the origin of the center-of-the-mass coordinate frame  $C_i^*$ .

If  $\mathbf{I}_i$  is the classical link inertia tensor about the center-of-mass of link  $i$ , the corresponding inertia tensor  $\mathbf{I}'_i$  about the link  $i$  coordinate frame  $C_i$  is computed

according to the parallel-axis theorem or Steiner's law:

$$\mathbf{I}'_i = \mathbf{I}_i + m_i (\mathbf{s}_i \mathbf{s}_i^T \mathbf{E} - \mathbf{s}_i \mathbf{s}_i^T) \quad (10)$$

where  $\mathbf{E}$  is the  $3 \times 3$  identity matrix. This transformation of the inertia tensor includes the quadratic terms of  $\mathbf{s}_i$ . When we substitute this in (6) in the Newton-Euler formulation, the quadratic terms from  $\mathbf{s}_i \times \mathbf{F}_i$  in (8) are absorbed in the transformation, thus resulting in the modified Newton-Euler dynamic formulation which is linear in center-of-mass vectors [9, 8].

Properties 1 and 2 together with this transformation lay the foundation for our identification algorithms, and Property 4 will be used to derive our off-line identification algorithm.

### 2.3. Torque/Force Error Model

In general, identification of all the link masses, dynamics parameters and the kinematic parameters is a problem of nonlinear estimation. If we assume that we have nominal values of those parameters, say from engineering drawings, we can linearize the torque/force equation of each link about the nominal values of the kinematic and dynamic parameters to obtain the torque/force error model [15]:

$$\epsilon_i = \tau_i - \tau_i^0 = \phi_i^T \Delta \psi_i \quad \text{for } i=1, 2, \dots, N \quad (11)$$

where  $\tau_i$  is the applied torque/force to link  $i$ ,  $\tau_i^0$  is the value of the torque/force, as computed by an inverse dynamics model using the nominal values [13],  $\epsilon_i$  is the input torque/force error of link  $i$ ,  $\Delta \psi_i$  is the correction vector of unknown parameters that affect the torque/force of link  $i$ , and  $\phi_i$  is the nonlinear vector function of the kinematic and dynamic parameters and the output measurements (joint positions, velocities and accelerations). The torque/force error model (11) relates the error torque/force of link  $i$  to corresponding modeling inaccuracies in the kinematic and dynamic parameters.

If we know the kinematic parameters (e.g., by measuring them) and the Newton-Euler model is transformed according to (10), then identification of the remaining dynamic parameters is a problem of linear estimation. The subject of estimating the kinematic parameters has been the focus of a lot of research and many algorithms have been proposed [17, 3, 6, 18]. In the sequel, we will assume that the kinematic parameters of the manipulator are known and the problem is one of estimating the dynamics parameters. Consequently, in (11)  $\phi_i$  is a function of only the known kinematic parameters and robot output measurements. Equation (11) is thus a linear equation with  $\mu_i$  unknowns, i.e.,  $\mu_i = \dim(\Delta \psi_i)$ . Because of the property 4, in Section 2.3, we can step sequentially through the links, from the tip to the base, and identify the dynamic parameters that affect the link torques/forces of each link. It must be noted, however, that all the parameters may

not be **always** identifiable, nor need be identified. That is, the number of independent dynamic parameters is less than or equal to the total number of dynamic parameters of a robot. This is explained in greater detail in Section 3.3.

#### 2.4. Example: Cylindrical Robot

We will illustrate the approach presented so far by using a three degrees-of-freedom cylindrical robot. We first develop its Newton-Euler dynamics model. After observing its properties, we apply the transformation of inertia tensor to obtain the equivalent modified Newton-Euler model. Finally the torque/force error model is developed.

The cylindrical robot consists of three degrees-of-freedom: a rotation  $\theta_1$ , a vertical translation  $d_2$  and a radial translation  $d_3$ . The Denavit-Hartenberg parameters of the cylindrical robot are:

Link	$\theta$	$\alpha$	$a$	$d$
1	$\theta_1$	$0^\circ$	0	0
2	0	$-90^\circ$	0	$d_2$
3	0	$0^\circ$	0	$d_3$

The coordinate vector of the cylindrical robot is thus  $\mathbf{q}=[\theta_1 \ d_2 \ d_3]^T$ . We assume that the classical link inertias of the three links are diagonal and that only the  $s_{1z}$ ,  $s_{2y}$  and  $s_{3z}$  components of the center-of-mass vectors **are** non-zero. These assumptions do not suffer from any **loss** of generality, and the cylindrical robot preserves all of the inherent coupling and nonlinear characteristics of robot dynamics.

We expand the Newton-Euler recursions (1)-(9) to obtain the complete dynamics model of the cylindrical robot:

$$\tau_3 = m_3 \ddot{d}_3 - m_3 (s_{3z} + d_3) \dot{\theta}_1^2 \quad (12)$$

$$\tau_2 = (m_2 + m_3) \ddot{d}_2 + (m_2 + m_3) g \quad (13)$$

$$\begin{aligned} \tau_1 = & [(I_{1zz} + I_{2yy} + I_{3yy}) + m_3 (s_{3z} + d_3)^2] \ddot{\theta}_1 \quad (14) \\ & + [2m_3 (s_{3z} + d_3)] \dot{d}_3 \dot{\theta}_1 \end{aligned}$$

We observe that equations (12)-(14) are linear in the classical link inertia tensor components, but nonlinear in the link center-of-mass vectors due to the presence of  $m_3 s_{3z}^2$  in (14). Also the dynamic parameters of link  $i$  **do** not affect the torques/forces of links  $i+1$  through 3.



Now the nonlinear transform in (10) for this cylindrical robot is given as,

$$I'_{3yy} = I_{3yy} + m_3 s_{3z}^2 \quad (15)$$

$$I'_{2yy} = I_{2yy} \quad (16)$$

$$I'_{1zz} = I_{1zz} \quad (17)$$

Upon substituting (15)-(17) into (12)-(14), we obtain the modified dynamics model:

$$\tau_3 = m_3 \ddot{d}_3 - m_3 (s_{3z} + d_3) \dot{\theta}_1^2 \quad (18)$$

$$\tau_2 = (m_2 + m_3) \ddot{d}_2 + (m_2 + m_3)g \quad (19)$$

$$\begin{aligned} \tau_1 = & [(I'_{1zz} + I'_{2yy} + I'_{3yy}) + m_3(2s_{3z} + d_3^2)] \ddot{\theta}_1 \\ & + [2m_3(s_{3z} + d_3)] \dot{d}_3 \dot{\theta}_1 \end{aligned} \quad (20)$$

We note that the nonlinearity  $m_3 s_{3z}^2$  in (14) has been absorbed by the transformation (15), and that  $I_{2yy}$  and  $I_{1zz}$  are retained. From this observation, we understand that once the nonlinearities associated with link  $i$  are identified in the dynamics model, we may proceed to transform the inertias of only link  $i$ .

Now the torque/force error models for the cylindrical robot are given by:

$$\epsilon_3 = \Delta(m_3 s_{3z})[-2\dot{\theta}_1^2] + \Delta m_3[\ddot{d}_3 - d_3 \dot{\theta}_1^2] \quad (21)$$

$$\epsilon_2 = \Delta(m_2 + m_3)[\ddot{d}_2 + g] \quad (22)$$

$$\begin{aligned} \epsilon_1 = & \Delta(I'_{1zz} + I'_{2yy} + I'_{3yy}) \ddot{\theta}_1 \\ & + \Delta(m_3 s_{3z})[2\ddot{\theta}_1 + 2\dot{d}_3 \dot{\theta}_1] + \Delta(m_3)[d_3^2 \ddot{\theta}_1 + 2d_3 \dot{d}_3 \dot{\theta}_1] \end{aligned} \quad (23)$$

In the above model the number of independent dynamic parameters are,  $\mu_3=2$  ( $m_3 s_{3z}$  and  $m_3$ : unknown),  $\mu_2=1$  ( $m_2$ : unknown), and  $\mu_1=1$  (because we can only identify the sum of the three inertias in (23), and the product  $m_3 s_{3z}$  and  $m_3$  have already been identified in (21)). We measure the input torque/force to link  $i$  and the position, velocity and acceleration of link  $i$  at  $N$  sampling instants (where  $N > \mu_i$ ), compute the nominal values of  $\tau_i^0$  (according to the inverse dynamics model in (18)-(20)), and apply the linear least-squares algorithm to estimate the dynamic parameters of link  $i$ .

### 3. Sequential Identification Procedures for an N-DOF Robot

In this section, we present the identification procedures for an  $N$  degree-of-freedom robot. We use the property 4 of the Newton-Euler formulation to simplify the derivation of the torque/force equations for the  $N$  links of the manipulator. We treat the parameter identification problem sequentially, starting from link  $N$  (the tip) and proceeding to link 0 (the base), and estimate the dynamic parameters of each link individually. The identified dynamic parameters of link  $i$  become known parameters in the torque/force equation of link  $i-1$ . This sequential procedure reduces the number of dynamic parameters which must be estimated from the torque/force error model of each link, and thus results in a robust identification procedure.

The identification of the dynamics parameters can be accomplished either off-line or on-line. In the off-line procedure, we collect all the input-output data prior to analysis and do not impose any limits on the computation time. In contrast, the on-line procedure deals with real-time updates of the parameters during robot operation and issue of computational requirements for estimation becomes important. In the following paragraphs, we present both the off-line and the on-line techniques for manipulator parameter estimation.

#### 3.1. Off-Line Identification Procedure

Since the dynamic parameters of the all the links except the payload are constant, we can estimate these parameters off-line. If we lock the first  $i-1$  joints mechanically (to set the velocities and accelerations of joints one through  $i-1$  to zero), we reduce dramatically the complexity of the torque/force error model of link  $i$ . This simplification can only be achieved in off-line estimation.

Off-line identification procedure for an  $N$  degree-of-freedom robot:

1. Expand the Newton-Euler recursive equations to obtain the closed-form link torques/forces equations of the manipulator. In deriving the torque/force equation for link  $i$ , set the velocities and accelerations of links 1 through  $i-1$  to zero.
2. Convert the Newton-Euler model into the modified (linear in dynamic parameters) Newton-Euler model, by applying the transformation (10) which transforms the classical inertias about the center-of-mass of link  $i$  to inertias about the  $i$ -th link frame.
3. Generate the torque/force error model (11) by incorporating the nominal values of the dynamic parameters to be estimated.
4. Calculate all of the Newton-Euler dynamic parameters in the torque/force error model that affect the torque/force of link  $i$ . Since the dynamic parameters affecting the torques/forces of links  $i+1$  through  $N$  have already been identified, these dynamic

parameters are known numerical quantities when working with link  $i$ .

### 3.2. On-line Identification Procedure

The on-line identification procedure for an  $N$  degree-of-freedom robot parallels steps 1 through 4 above, but in deriving the torque/force equations in Step 1 we allow positions, velocities and accelerations of links  $i-1$  through 1 to respond to the actuating torques/forces instead of setting them to zero,

### 3.3. Identifiable Parameters

Each link of a robot is characterized by a maximum of ten dynamic parameters: the link mass, the six classical inertias and the three elements of the center-of-mass vector. In practice, only a fraction of the ten parameters of link  $i$  and a fraction of the  $10(N-i)$  dynamic parameters of links  $i+1$  through  $N$  affect the torque/force  $\tau_i$  of link  $i$ . We emphasize that we can only estimate (and need to estimate) the dynamic parameters that actually affect the joint torques/forces. For example, the  $I_{3xx}$  classical moment-of-inertia parameter of the cylindrical robot does not affect the dynamic robot model in (12)-(14) and hence cannot be identified.

The estimation of the classical inertias may not be unique and only their linear combinations may be identified. For example, equation (23) allows us to estimate only the sum  $I'_{1zz} + I'_{2yy} + I'_{3yy}$  of the link inertias. Such an estimate is sufficient for computing the closed-form inverse dynamics in (18)-(20). If, however, the inverse dynamics are implemented by the original recursive Newton-Euler formulation in (1)-(9), the numerical values of all of the classical link inertias are required. For this purpose, we can set the values of first two of the three classical link inertias to zero, and set the third to the value of the estimated sum. Even though this particular assignment of numerical values may not have physical significance, it does lead to the arithmetically-correct computation of the torque/force.

The closed-form dynamic model of a *six* degree-of-freedom robot is in general very complex, and the corresponding torque/force error model for on-line estimation of all the robot parameters including payload characteristics is of comparable complexity. To facilitate the estimation process, a viable strategy is to identify the parameters of all the links first by the off-line procedure and to estimate on-line the mass and the inertial characteristics of the payload. This strategy requires the real-time identification of only the last link of the robot. Our identification algorithm is directly amenable to the real-time identification of the payload characteristics for dynamic feedback control.

### 3.4. Parameter Identifiers

In sections 5.1 and 5.2, we have developed the torque/force error models. We now need to cast these models into parameter identifier structures. A parameter identifier consists of three components: the system to be identified, a postulated model, and an adaptation algorithm which updates the model based upon an error criterion. In our case, the system is the physical robot and the model is the Newton-Euler inverse arm dynamics model. The inputs to the robot are the joint torques/forces and the outputs are the joint positions, velocities, and accelerations. The inputerror structure for identification is shown in Figure 1 wherein the outputs of the robot are fed to the inverse arm dynamics model which computes the joint torques/forces. The error signal, which is the difference between the applied and the computed torques, drives the estimation algorithm.

Often times it is desired to evaluate the robustness of the estimation algorithms through simulation studies before the experimental implementation. Although the input-error structure can be used for these practical studies, its implementation is computation intensive due to the forward arm simulation. We thus introduce the outputerror structure, depicted in Figure 2, for simulation studies. In this structure the difference between the output torques/forces of the system and the model is the error signal which drives the identification algorithm. Since the error signal (which is the difference between the system and the model torques/forces) is identical in both the input-error and output-error identifier structures they accommodate identical estimation algorithms. This is a practical advantage because the applicability and performance of an on-line estimation algorithm can be evaluated through off-line simulation studies.

## 4. Simulation Results

We have performed simulation experiments for identifying the dynamic parameters of the cylindrical robot and the three degrees-of-freedom CMU DD Arm II. We commanded each joint to move in a sinusoidal trajectory, beginning from the rest position to a ninety degree position and returning in one second. We sampled the trajectory at 20-ms intervals and used the first half of the trajectory (or 25 sample points) in our identification experiments. One data point consists of the measurements of the applied torque/force and the position, velocity and acceleration of a link. Since we estimate only the dynamics parameters, the problem is linear and we have applied the least-squares algorithm under the assumption that the input-output measurements were noise-free. This assumption is justified practically by the current availability of high resolution resolvers (16 bits/revolution) and tachometers [7].

### 4.1. Cylindrical Robot

In Table 2, we summarize our simulation results for the cylindrical robot. We implemented the least-squares algorithms for the torque/force error model in (20) of the third link using the 25 data sets and identified the z-component of the center-of-mass

Figure 1: Input-error structure for parameter identification

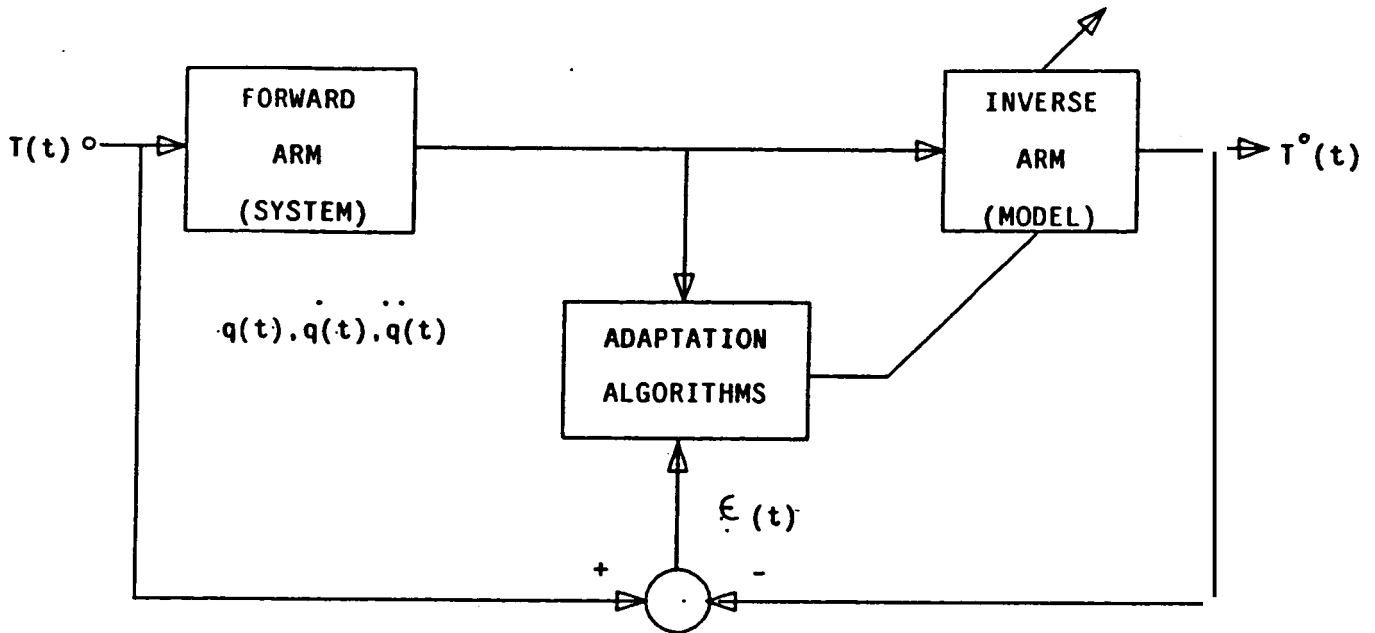
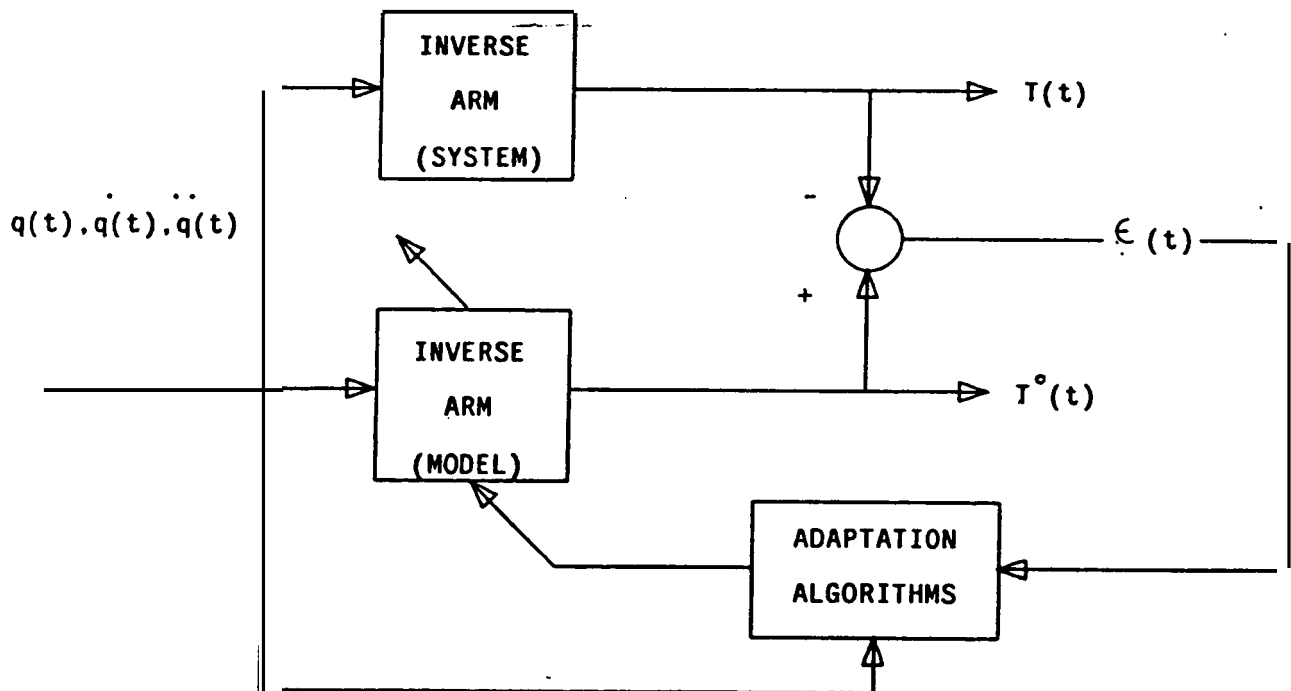


Figure 2: Output-error Structure for Parameter Identification



vector of the third link  $s_{3z}$ . We then identified the sum of the link inertias from the

torque/force error model of the first link by again using the 25 data sets **along** the trajectory. The estimated values match exactly the true values.

**Table 2: Simulation Results for the Cylindrical Robot**

Link	Dynamic Parameter (Dimensions)	Initial Value	True Value	Estimated Value
3	$m_3 s_{3z}$ (m)	0.27	1.25	1.249
	$m_3$ (kg)	0.9	2.5	2.499
2	$m_2$ (kg)	2.1	5.0	5.000
1	$I_{1zz} + I_{2yy} + I_{3yy}$ (kg-m <sup>2</sup> )	2.0	2.5	2.5

#### 4.2. CMU Direct-Drive Arm II

The configuration of the CMU DD Arm II is shown in Figure 3. Throughout this experiment, we assume that the Denavit-Hartenberg or the kinematic parameters of the CMU DD Arm II are known.

**The** torque/force error model of the 3 DOF positioning system of the CMU DD Arm II is described the following equations:

$$\begin{aligned}
\epsilon_3 = & \Delta(I_{3xz})[\dot{\theta}_1^2 - 2C_3\dot{\theta}_1^2 + 2\dot{\theta}_1\dot{\theta}_2 - 4C_3^2\dot{\theta}_1\dot{\theta}_2 + \dot{\theta}_2^2 - 2C_3^2\dot{\theta}_2^2] \\
& + \Delta(I_{3yz})[-C_3\ddot{\theta}_2 - C_3\ddot{\theta}_1] + \Delta(I_{3yy})[\ddot{\theta}_3] \\
& + \Delta(I_{3zz} - I_{3xx})[2C_3S_3\dot{\theta}_1\dot{\theta}_2 + C_3S_3\dot{\theta}_1^2 + C_3S_3\dot{\theta}_2^2] \\
& + \Delta(I_{3xy})[-S_3\ddot{\theta}_2 - S_3\ddot{\theta}_1] \\
& + \Delta(m_3s_{3z})[-d_3C_3\ddot{\theta}_2 - d_3C_3\ddot{\theta}_1 - gS_3 + a_1C_2C_3\dot{\theta}_1^2 \\
& - a_1C_3S_2\ddot{\theta}_1 + a_2C_3\dot{\theta}_2^2 + 2a_2C_3\dot{\theta}_1\dot{\theta}_2 + a_2C_3\dot{\theta}_1^2] \\
& + \Delta(m_3s_{3x})[-d_3S_3\ddot{\theta}_2 - d_3S_3\ddot{\theta}_1 + gC_3 + a_1C_2S_3\dot{\theta}_1^2 \\
& - a_1S_3S_2\ddot{\theta}_1 + a_2S_3\dot{\theta}_2^2 + 2a_2S_3\dot{\theta}_1\dot{\theta}_2 + a_2S_3\dot{\theta}_1^2]
\end{aligned} \tag{24}$$

$$\begin{aligned}
\epsilon_2 = & \Delta(I_{2yy})[\ddot{\theta}_1 + \ddot{\theta}_2] + \Delta(I_{3zz})[C_3^2\ddot{\theta}_2 + C_3^2\ddot{\theta}_1] \\
& + \Delta(I_{3xx})[S_3^2\ddot{\theta}_2 + S_3^2\ddot{\theta}_1] \\
& + \Delta(m_2s_{2x})[2a_2\ddot{\theta}_1 + a_1C_2\ddot{\theta}_1 + a_1S_2\dot{\theta}_1^2 + 2a_2\ddot{\theta}_2] \\
& + \Delta(m_2s_{2z})[-a_1C_2\dot{\theta}_1^2 + a_1S_2\ddot{\theta}_1] \\
& + \Delta(m_3s_{3y})[a_1C_2\dot{\theta}_1^2 - a_1S_2\ddot{\theta}_1 - 2d_3\ddot{\theta}_2 - 2d_3\ddot{\theta}_1] \\
& \Delta(m_2)[(a_1a_2C_2 + a_2^2)\ddot{\theta}_1 + a_2^2\ddot{\theta}_2] \\
& \Delta(m_3)[(a_1d_3S_2 + d_3^2 + a_1a_2C_2 + a_2^2)\ddot{\theta}_1 + (d_3^2 + a_2^2)\ddot{\theta}_2]
\end{aligned} \tag{25}$$

$$\epsilon_1 = \Delta(I_{1zz})\ddot{\theta}_1 + \Delta(m_1s_{1x})2a_1\ddot{\theta}_1 + \Delta(m_1)[a_2^2\ddot{\theta}_1] \tag{26}$$

where  $C_i = \cos\theta_i$  and  $S_i = \sin\theta_i$ .

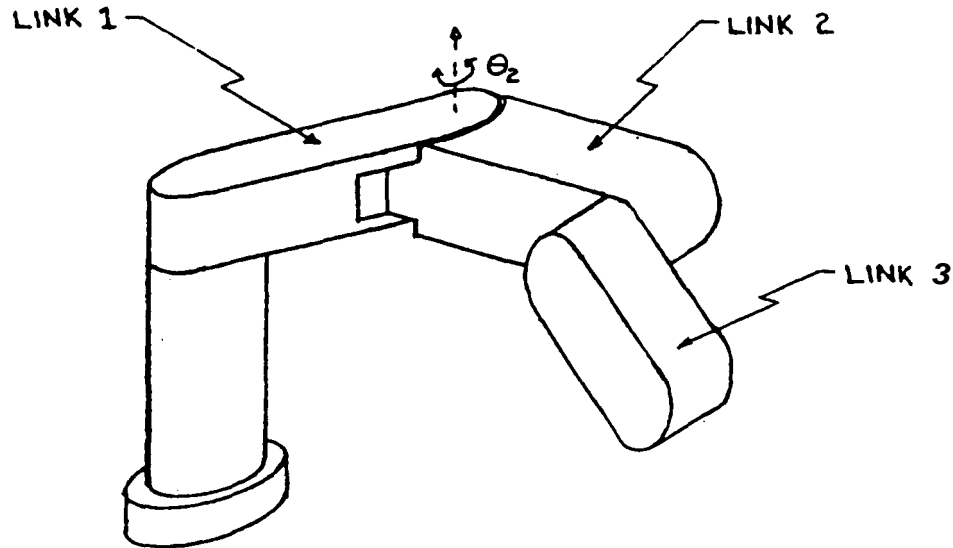
From these equations, we observe that:

- The torque of the third link is affected by all the elements of the inertia matrix and also by the two elements,  $s_{3x}$  and  $s_{3z}$ , of the center-of-mass vector. However, we can only identify seven of the eight parameters in (24) because the inertia elements  $I_{3xx}$  and  $I_{3zz}$  occur as a linear combination.
- The torque of link 2 is affected by two inertia elements and the mass of the third link, one inertia element and the mass of the second link, two elements of the center-of-mass vector of the second link and one element of the center-of-mass vector of the third link. All these parameters occur independently and can be uniquely identified. Note that we could identify only the linear combination  $I_{3zz} - I_{3xx}$  from the torque/force error model of the third link whereas we can identify  $I_{3zz}$  and  $I_{3xx}$  independently from the torque/force error model of the second link.
- The torque of the first link is affected by three independent dynamic parameters,  $I_{1zz}$ ,  $m_1$  and  $s_{1x}$ , which can be identified uniquely.

In summary, for the three degree-of-freedom positioning system of the CMU DD Arm II, we can identify seventeen of the twenty-seven unknown dynamic parameters.

The results of our simulation experiments for the CMU DD Arm II are summarized in Table 3. We used the 25 data sets to identify successfully the dynamic parameters which affect the torques/forces of each of the three links.

Figure 3: Kinematic configuration of the CMU DirectDrive Arm II



## 5. Experimental Implementation

Experimental implementation of the identification algorithm requires the knowledge of the applied joint torques and the measured joint positions, velocities and accelerations. Each joint of the DD Arm II is instrumented to measure the position and the velocity. The applied joint torques are assumed to be the same as the torques computed from the control law. This assumption is valid because we use current controlled servo motors and has also been verified by experimentation [8]. Further, the joint acceleration is obtained by differentiating the measured velocity.

### 5.1. Obtaining the Joint Acceleration

The operation of obtaining the derivative of a set of data is inherently noisy because the differentiator essentially behaves like a high pass-filter. And this effect is further accentuated if the measured data is known to have some noise. In such a circumstance a commonly used method is to low-pass filter the measured data and then differentiate the resultant signal. This procedure serves to reduce the noise in the differentiated signal at the cost of incorporating a phase shift and hence the loss of fidelity.

Another method involves using the principle of least-squares for solving the problem of differentiation [11]. In this method, the differentiating filter is designed by fitting a second-order parabola to five consecutive points with the assumption that the derivative



Table 3: Simulation Results for the CMU DD Arm II

Link	Parameter (Dimensions)	Initial Value	True Value*	Estimated Value
3	$I_{3xz}$ (kg-m <sup>2</sup> )	0.0	0.1	0.1
	$I_{3yz}$ (kg-m <sup>2</sup> )	0.0	0.15	0.15
	$I_{3yy}$ (kg-m <sup>2</sup> )	0.0	0.2	0.1999
	$I_{3xy}$ (kg-m <sup>2</sup> )	0.0	0.15	0.15
	$I_{3zz} - I_{3xx}$ (kg-m <sup>2</sup> )	0.0	0.1	0.1
	$m_3 s_{3x}$ (m)	0.0	0.49	0.4898
	$m_3 s_{3z}$ (m)	0.0	0.7	0.7002
2	$I_{2yy}$	0.3	0.5	0.4999
	$I_{3xx}$ (kg-m <sup>2</sup> )	0.05	0.2	0.2001
	$I_{3zz}$ (kg-m <sup>2</sup> )	0.1	0.3	0.3001
	$m_2 s_{2x}$ (m)	0.4	1.1	1.1
	$m_2 s_{2z}$ (m)	0.0	0.55	0.55
	$m_3 s_{3y}$ (m)	0.2	0.525	0.5251
	$m_2$ (kg)	4.0	5.5	5.4999
	$m_3$ (kg)	2.0	3.5	3.501
1	$I_{1zz}$ (kg-m <sup>2</sup> )	1.0	1.3	1.2999
	$m_1 s_{1x}$ (m)	0.00	2.7	2.7013
	$m_1$ (kg)	10.0	13.5	13.5

(\*) These values are hypothetical figures for simulation, and do not correspond to those of the real CMU DD Arm II.

does not change much during the period of the observations. This assumption is especially true since we sample the position and the velocity of the joints every 2 ms. As the five data points, in general, cannot be guaranteed to lie on a second-order curve, we obtain the coefficients of the parabola by using the principle of least-squares. The resulting filter is described by the following difference equation:

$$f'(x) = \frac{-2f(x-2T) - f(x-T) + f(x+T) + 2f(x+2T)}{10T} .$$

where the symbol  $'$  denotes the derivative and  $T$  is the sampling period in seconds. The above filter obtains the derivative of the function  $f(x)$  at the point  $x$  by using the two immediate neighbors on both sides and thus represents a noncausal operation for real-time implementation. However, if we are able to tolerate a delay of two sampling periods then the filter can be made causal by shifting the data by two sampling instants to obtain:

$$f'(x-2T) = \frac{-2f(x-4T) - f(x-3T) + f(x-T) + 2f(x)}{10T}$$

In the off-line implementation of our identification algorithm, the noncausal nature of the filter presents no problem as all the data is known in advance. In order to obtain the joint acceleration from the measured joint velocity, we experimented with many methods of implementing differentiating filters and found the filter designed on the basis of the principle of least-squares to possess superior noise rejection properties. Consequently, we used this differentiating filter to estimate the the acceleration of the joints.

## 5.2. Trajectory Selection

One of the important constituents of identification is the selection of input trajectories for exciting the system. The input trajectory must be such that it allows complete identification of the system. Such a trajectory is known as a *persistently exciting* trajectory [5]. Choosing a persistently exciting trajectory is sufficiently complex and has not been addressed in this research. However, a method to determine if a chosen trajectory is persistently exciting is presented in [8]. In the experimental implementation, we used this method to ensure that the trajectories chosen for identification of the dynamics parameters were persistently exciting.

## 5.3. Experimental Results

We have implemented our identification algorithm together with the differentiating filter and obtained the estimates of the dynamics parameters of the CMU Direct-Drive Arm II. The modeled values of the dynamics parameters were chosen to be the initial estimates and the data of a sample trajectory run recorded. We then estimated the dynamics parameters based on our algorithm, and these are depicted in Tables 4, 5, and 6.

The identification experiments were performed with two different persistently exciting

Table 4: Experimental Results for the CMU DD Arm II

Link	Parameter (Dimensions)	Initial Value	Estimated Value
6	$I_{6xx}$ (kg-m <sup>2</sup> )	0.000426	0.002092
	$I_{6xy}$ (kg-m <sup>2</sup> )	0.0	0.000011
	$I_{6xz}$ (kg-m <sup>2</sup> )	0.0	0.000022
	$I_{6yy}$ (kg-m <sup>2</sup> )	0.000421	0.001979
	$I_{6yz}$ (kg-m <sup>2</sup> )	0.0	0.000010
	$I_{6zz}$ (kg-m <sup>2</sup> )	0.000047	0.000310
	$m_6 s_{6x}$ (m)	0.0	-0.000090
	$m_6 s_{6y}$ (m)	0.0	-0.000187
	$m_6 s_{6z}$ (m)	0.002199	0.008709
	$m_6$ (kg)	0.269	0.90018
5	$I_{5xx}$ (kg-m <sup>2</sup> )	0.002018	0.002602
	$I_{5xy}$ (kg-m <sup>2</sup> )	0.0	0.000302
	$I_{5xz}$ (kg-m <sup>2</sup> )	0.0	-0.000108
	$I_{5yy}$ (kg-m <sup>2</sup> )	0.001049	0.001349
	$I_{5yz}$ (kg-m <sup>2</sup> )	-0.000092	-0.000070
	$I_{5zz}$ (kg-m <sup>2</sup> )	0.001396	0.001211
	$m_5 s_{5x}$ (m)	0.0	0.000981
	$m_5 s_{5y}$ (m)	0.005130	0.006744
	$m_5 s_{5z}$ (m)	-0.016784	-0.019689
	$m_5 + m_4$ (kg)	2.817	3.0895

Table 5: Experimental Results for the CMU DD Arm II (contd.)

Link	Parameter (Dimensions)	Initial Value	Estimated Value
4	$I_{4xx}$ (kg-m <sup>2</sup> )	0.023775	0.030765
	$I_{4xy}$ (kg-m <sup>2</sup> )	0.0	-0.00100
	$I_{4xz}$ (kg-m <sup>2</sup> )	0.0	0.000302
	$I_{4yy}$ (kg-m <sup>2</sup> )	0.004055	0.003655
	$I_{4yz}$ (kg-m <sup>2</sup> )	0.003083	0.004207
	$I_{4zz}$ (kg-m <sup>2</sup> )	0.021652	0.029002
	$m_4 s_{4x}$ (m)	0.0	-0.002402
	$m_4 s_{4y}$ (m)	0.134764	0.160372
	$m_4 s_{4z}$ (m)	0.043011	0.081462
3	$I_{3xx}$ (kg-m <sup>2</sup> )	0.014622	0.015192
	$I_{3xy}$ (kg-m <sup>2</sup> )	0.0	0.000726
	$I_{3xz}$ (kg-m <sup>2</sup> )	0.0	0.000109
	$I_{3yy}$ (kg-m <sup>2</sup> )	0.006615	0.006209
	$I_{3yz}$ (kg-m <sup>2</sup> )	0.001269	0.001872
	$I_{3zz}$ (kg-m <sup>2</sup> )	0.012432	0.014080
	$m_3 s_{3x}$ (m)	0.0	0.015242
	$m_3 s_{3y}$ (m)	-0.039703	-0.132251
	$m_3 s_{3z}$ (m)	-0.012487	-0.040521
	$m_3$ (kg)	2.801	2.92106

Table 6: Experimental Results for the CMU DD Arm II (contd.)

Link	Parameter (Dimensions)	Initial Value	Estimated Value
2	$I_{2yy}$ (kg-m <sup>2</sup> )	0.264736	0.322156
	$m_2 s_{2x}$ (m)	-1.039971	-1.156482
	$m_2 s_{2z}$ (m)	0.008722	0.008234
	$m_2$ (kg)	7.894	8.2501
1	$I_{1zz}$ (kg-m <sup>2</sup> )	1.193645	1.270784
	$m_1 s_{1x}$ (m)	-5.925900	-6.478305
	$m_1$ (kg)	19.753000	20.152630

trajectories and two sets of initial values for the modeled dynamics parameters. In all the four experiments, the estimated values of the dynamics parameters were found to be within **5%** of the values depicted in Tables 4 through 6. This variation is practically negligible and may be attributed to the noise in the measurements which tends to bias the estimates, and **also** to the errors in the kinematic parameters which also have a similar effect.

## 6. Conclusion

In this paper, we have addressed the problem of robot dynamics parameter identification and applied our algorithm to experimentally determine the dynamics parameters of CMU Direct-Drive Arm II. Since the CMU DD Arm II has negligible friction it was not modeled in the estimation algorithm. However, this may not be the case in non-direct drive manipulators and the friction would have to be modeled. If the friction is modeled **as** a linear function of the joint velocity then the estimation problem will still be linear. In practice the linear approximation may be inadequate and the friction might have to be modeled **as** a nonlinear function. In such a case the estimation problem becomes nonlinear and more complicated.

In deriving our estimation algorithm **we** noted that some dynamic parameters do **not** appear in the joint torque/force equations and others appear in linear combinations. Since we don't sense the full torque/force vector at each joints, we can identify only those parameters which affect the joint torque/force. Based on this observation, we classify the parameters in three categories: those that can be uniquely identified, those that can be

identified only in linear combinations, and those which cannot be identified. It is imperative that the parameters that can be identified only **as** linear combinations be singled out and this knowledge be incorporated in the identification procedure, so that the numerical procedure, such **as** the least-square error, to compute the parameter values, becomes stable and robust. Incorporating this knowledge in the inverse dynamics formulation also reduces its computational requirements. A systematic procedure for the parameter categorization is further developed in [10, 8].

## References

- [1] **An, C. H.**, Atkeson, C. G. and Hollerbach, J. M.  
Estimation of Inertial Parameters of Rigid Body Links of Manipulators.  
In *Proceedings of the 24-th CDC*. **1985**.
- [2] Brady, M., et al. (editors).  
*Robot Motion: Planning and Control*.  
MIT Press, Cambridge, MA, **1982**.
- [3] Chen, J., Wang, C. B. and Yang, C. S.  
Robot Positioning Accuracy Improvement through Kinematic Parameter  
Identification.  
In *Proceedings of the Third Canadian CAD/CAM in Robotics Conference*.  
pages **4.7-4.12**, Toronto, Canada, June, **1984**.
- [4] Coiffet, **P.**  
*Robot Technology. Volume 2: Interaction With the Environment*.  
Prentice-Hall, NJ, **1983**.
- [5] Goodwin, G. C. and Sin, K. S.  
*Adaptive Filtering, Rediction and Control*.  
Prentice-Hall, Englewood-Cliffs, NJ, **1984**.
- [6] Hayati, S. and Mirmirani, **M.**  
Puma 600 Robot Calibration.  
In *Proceedings of the First IEEE International Conference on Robotics and  
Automation*. **IEEE**, Atlanta, GA, March, **1984**.
- [7] Kanade, T., Khosla, P. K. and Tanaka, N.  
Real-Time Control of the CMU Direct Drive Arm II Using Customized Inverse  
Dynamics.  
In Polis, M. P. (editor), *Proceedings of the 23rd IEEE Conference on Decision  
and Control*, pages **1345-1352**. Las Vegas, NV, December **12-14**, **1984**.
- [8] Khosla, P. K.  
Real-Time Control and Identification of Direct-Drive Manipulators.  
PhD Thesis, Department of Electrical and Computer Engineering, Carnegie-Mellon  
University, August **1986**.
- [9] Khosla, P. K. and Kanade, T.  
Parameter Identification of Robot Dynamics.  
In Franklin, G. F. (editor), *Proceedings of the 24-th CDC*, pages **1754-1760**.  
Florida, December **11-13**, **1985**.

- [10] Khosla P. K. and Kanade, T.  
*An Algorithm to Determine the Identifiable Parameters in the Dynamic Robot Model.*  
Vision Lab Report **RVL-031**, The Robotics Institute, Carnegie-Mellon University,  
May, **1985**.
- [11] Lanczos, C.  
*Applied Analysis.*  
Prentice Hall Inc., Englewood Cliffs, N. J., **1956**.
- [12] Luh, J. Y. S., Walker, M. W. and Paul, R. P.  
Resolved-Acceleration Control of Mechanical Manipulators.  
*IEEE Transactions on Automatic Control* **25(3):468-474**, June, **1980**.
- [13] Luh, J. Y. S., Walker, M. W. and Paul, R. P.  
On-Line Computational Scheme for Mechanical Manipulators.  
*Journal of Dynamic Systems, Measurement, and Control* **102(2):69-76**, June,  
**1980**.
- [14] Markiewicz, B. R.  
*Analysis of the Computed-Torque Drive Method and Comparison with the  
Conventional Position Servo for a Computer-Controlled Manipulator.*  
Technical Memorandum **33-601**, Jet Propulsion Laboratory, Pasadena, CA, March,  
**1973**.
- [15] Neuman, C. P. and Khosla, P. K.  
Identification of Robot Dynamics: An Application of Recursive Estimation.  
In Narendra, K. S. (editor), *Proceedings of the Fourth Yale Workshop on  
Applications of Adaptive Systems Theory*, pages **42-49**. Yale University, New  
Haven, CT, May **29-31, 1985**.
- [16] Paul, R. P.  
*Robot Manipulators - Mathematics, Programming and Control.*  
MIT Press, Cambridge, MA, **1981**.
- [17] Stone, H. W., Sanderson, A. and Neuman, C. P.  
Arm Signature Identification.  
In *Proceedings of the 1986 IEEE Conference on Robotics and Automation.*  
IEEE, San Francisco, CA, April, **1986**.
- [18] Whitney, D. and Lozinski, C. A.  
Industrial Robot Calibration Methods and Results.  
In *Proceedings of the International Computers in Engineering Conference.*  
ASME, Atlanta, GA, August, **1984**.